A New High-Efficiency Optical–Microwave Mixing Approach

Gábor Járó, *Member, IEEE*, and Tibor Berceli, *Fellow, IEEE*

***Abstract*—High sensitivity reception is a crucial problem of fiber radio links. A significant improvement is obtained by applying a new approach called optical–microwave double mixing. The new approach can provide as much as 30 dB of higher mixing product in a narrow-band compared with the direct detection applying only additional passive components. Detailed investigation of the optical–microwave double-mixing method is shown to get optimum adjustment for specific applications. The new method is advantageously used for the reception of subcarrier-multiplexed optical signals.**

***Index Terms*—Fiber radio, optical–microwave mixing, optical reception, subcarrier-multiplexed optical transmission.**

I. Introduction

THE widely used optical receivers mainly apply photodiodes (PDs) to detect the optical intensity-modulated signal. A relatively high sensitivity is achieved by properly matched transimpedance or distributed amplifiers [1]–[3]. In another method, the modulated optical signal is mixed with a microwave signal in the PD, producing an intermediate frequency signal [4]–[11]. Thus, heterodyne-type reception is feasible. However, the mixing conversion has a higher loss compared with the direct detection.

In the new optical–microwave double-mixing approach, the conversion loss is much less than that of the direct detection, offering a significant improvement in the reception sensitivity. The mixing product is even further increased by resonance enhancement, providing 30 dB of total improvement in comparison with direct detection.

The mixing process can be compared with the direct detection, considering not only the received signal power but also other aspects as well. In the case of mixing, the received signal is not in the baseband but at an intermediate frequency (IF). That results in a narrower relative bandwidth (with the same absolute bandwidth). At intermediate frequencies, a lower noise figure is feasible compared with the baseband reception. The transmission characteristics (such as amplitude and phase response) are improved because of the smaller relative bandwidth. In the IF band, the selection of the subcarrier channels is also easier compared with the baseband reception.

Manuscript received April 15, 2003; revised September 16, 2003. This work was supported in part by the Commission of the European Union under the LABELS and NEFERTITI projects and by the Hungarian National Scientific Research Foundation under OTKA T-026557, T-030148, and T-042557.

G. Járó was with the Department of Broadband Infocommunication Systems, Budapest University of Technology and Economics, H-1111 Budapest, Hungary. He is now with Nokia Hungary, Budapest, Hungary (e-mail: gabor.jaro@nokia.com).

T. Berceli is with the Department of Broadband Infocommunication Systems, Budapest University of Technology and Economics, H-1111 Budapest, Hungary (e-mail: tibor.berceli@mht.bme.hu).

Digital Object Identifier 10.1109/JLT.2003.819782

II. Double-Mixing Principle

In the conventional optical–microwave mixing process, an intensity-modulated optical signal and a microwave signal are applied to a nonlinear high-speed optical device e.g., a p-i-n PD that is sensitive both for optical and microwave signals. Due to the nonlinear behavior of the device, mixing products are generated, i.e., the upper and lower sidebands of the microwave signal appear at the output. One of these mixing products is used for reception. However, the conversion loss of the optical–microwave mixing is significantly higher than the conversion loss of the direct optical detection. Therefore, the optical–microwave mixing has limited application, although it has many advantages from other viewpoints, e.g., selectivity, noise, and relative bandwidth.

Based on our investigations, we noticed that besides the optical–microwave mixing, there is a photodetection process as well. However, presently, the detected signal is not utilized in the mixing procedure. Our new idea is that the photodetected signal should also be utilized somehow. Therefore, we developed a new method for the utilization of the detected signal in the mixing process: by a proper embedding circuit, the detected signal is reflected back into the nonlinear device, and this way, it is mixed again with the microwave signal. In case of phase coherence, the two mixing products are added constructively and, thus, the output signal is increased significantly. We call that method optical–microwave double mixing because it simultaneously utilizes two effects: a direct and an indirect mixing process of the modulated optical signal and the microwave signal. As a result of the application of the double-mixing method, 10–15-dB improvement is obtained compared with the conventional mixing approach.

The mixing product can be even further increased by an additional resonance enhancement approach. The resonant enhancement method is already widely used in case of narrow-band applications. It can be used for Mach–Zehnder modulators (MZMs), photodetectors, etc. This way, an additional 10–15-dB increase in the output signal can be achieved. For example, in the case of MZMs, the electrodes of the microwave driving circuit can have a resonant structure. The result is an increase in the modulation depth. The MZM can also be used for optical–microwave mixing. However, its conversion loss is much higher than the conversion loss of simple p-i-n diode mixing. Usually, the conversion loss of the Mach–Zehnder mixer is 20–25 dB higher. By the application of the resonant enhancement, the mixing product of the MZM

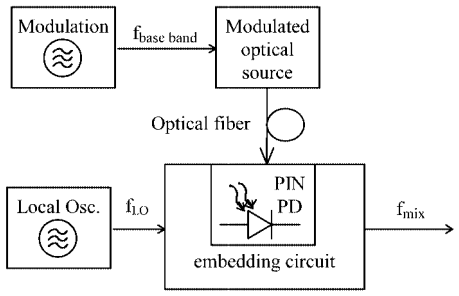

Fig. 1. Optical–microwave mixing setup.

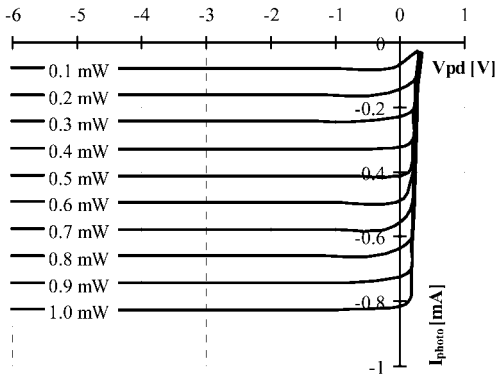

Fig. 2. Measured dc characteristic of the p-i-n PD (parameter is the incident optical power).

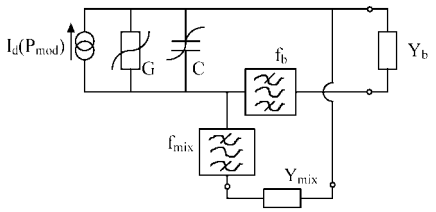

Fig. 3. p-i-n diode simplified circuit model for double mixing.

is increased by 10–15 dB; nevertheless, it is still 10–15 dB higher than the mixing product of simple p-i-n mixing without resonant enhancement.

III. Investigation of the Double-Mixing Process

The setup of the optical–microwave circuit is shown in Fig. 1. The intensity-modulated optical signal illuminates the PD which is in an embedding electrical circuit. The embedding circuit can be optimized for detection or mixing.

The measured dc characteristics of the 1A358 type MITEL CATV p-i-n PD is shown in Fig. 2. Here, the detected photocurrent is plotted as a function of the bias voltage for different illumination intensities.

For the investigation of the double-mixing process, the simplified model of Fig. 3 is used. Here, the p-i-n PD is represented by a current source, providing the effect of illumination, a nonlinear conductance G, and a nonlinear capacitance C. The baseband signals $\sqrt{f_b}$ and the mixing products $\sqrt{f_{\rm mix}}$ are separated by branching filters, and they are terminated by the admittances Y_b and $Y_{\rm mix}$. Based on Fig. 3, it is seen that the current of the detected optical signal flows through the admittance Y_b, and when reflected back, it develops an additional voltage across the terminals of the PD. This signal is also mixed with the microwave signal producing a mixing product as well. The two mixing products, the results of two effects, are added if they are in phase and subtracted when the phase difference between them is 180°. Applying a resonant circuit in the baseband, the effect is enhanced, increasing the mixing product very significantly.

The mixing process is explained as a result of the nonlinear current-voltage relationship [12]–[18]. The detected lightwave is characterized by an equivalent photo-voltage. Due to the strong nonlinearity, the mixing product is generated by the microwave driving voltage and the photo-voltage. The I–V characteristics of a biased p-i-n PD under illumination is described by an exponential function

$$I = I_0 \left[\exp\left(\frac{V}{V_T}\right) - 1 \right] - I_{\rm opt} \tag{1}$$

where V_T is the thermal voltage of the diode, and $I_{\rm opt}$ is the photocurrent.

The voltage of the diode V can be expressed as a sum of the voltages

$$V = V_{\rm dc} + V_{\rm LO} + V_{\rm mod} \tag{2}$$

where $V_{\rm dc}$ is the dc-bias point of the diode, and $V_{\rm LO}$ and $V_{\rm mod}$ are the local oscillator (LO) and the modulation signals, respectively. $V_{\rm mod}$ can be expressed as a function of the modulated optical power $(P_{\rm mod})$, the responsivity of the diode $R(V)$ at the actual bias, and the termination impedance in the baseband $Z_{\rm mod}$

$$V_{\rm mod} \approx P_{\rm mod} R(V) Z_{\rm mod}. \tag{3}$$

Substituting the latter (1)–(3) into each other, the ac current of the PD is described as the multiplication of two functions

$$\Delta I \cong F_1(V_{\rm LO}) F_2(P_{\rm mod}) \tag{4}$$

where F_1 is dependent on the applied LO signal, and F_2 is only dependent on the intensity of the light. Both F functions are dependent on the bias voltage.

The aim is to investigate high-frequency signals. Therefore, the two functions in the (4) are approximated by their Taylor series

$$\begin{aligned} F_1(V) \cong & F_1(V_0) \\ & + \left.\frac{dF_1(V)}{dV}\right|_{V_0} \Delta V + \frac{1}{2} \left.\frac{d^2F_1(V)}{dV^2}\right|_{V_0} \\ & \times \Delta V^2 + \cdots \\ F_2(P) \cong & F_2(P_0) \\ & + \left.\frac{dF_2(P)}{dP}\right|_{P_0} \Delta P + \frac{1}{2} \left.\frac{d^2F_2(P)}{dP^2}\right|_{P_0} \\ & \times \Delta P^2 + \cdots. \end{aligned} \tag{5}$$

The proper combinations of these F functions (5) produce the up-converted signals, including the higher order distortions as well.

As it can be seen in Fig. 2, the current-voltage curves contain three different sections in case of illumination. At low positive

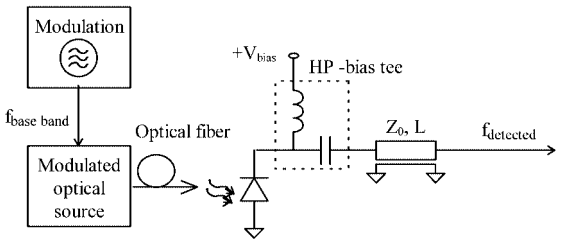

Fig. 4. Detection measurement setup.

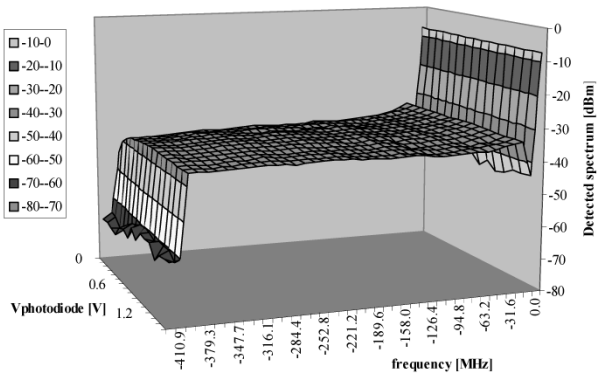

Fig. 5. Detected spectrum (-35.83 dBm @ 200 MHz and 1.5-V reverse bias).

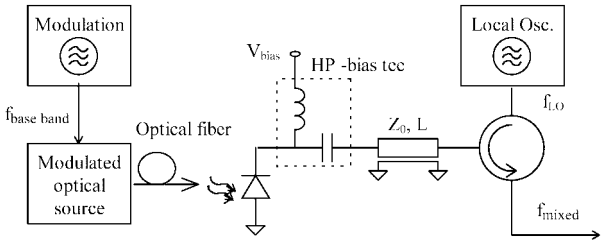

Fig. 6. Mixing measurement setup with real circulator.

voltages, the current changes very suddenly with small voltage changes, and the responsivity of the PD is very small caused by the high transit time of the diode. Then, a sharp knee is obtained where the nonlinearity of the characteristics is still high and the responsivity is higher caused by the increased reverse-bias voltage. After the knee point, the current is almost saturated, and the device is rather linear. In this region, the responsivity of the diode is the highest so that it can be used for optical detection.

The mixing efficiency depends on the responsivity of the diode and the nonlinearity of the characteristics. Because the photo-voltage and the nonlinearity change in the opposite direction as a function of the reverse-bias voltage, the highest mixing product can be generated using a bias close to the knee point of the dc curve. In case of the MITEL 1A358 PD, the optimum bias point for optical–microwave mixing is in the range -0.2 V $\ldots -0.3$ V (reverse bias), as it will be shown in the figures presenting measured results. The bias sensitivity of the maximum mixing product is not high. By a simple stabilization of the bias voltage, this maximum can be kept unchanged. For example, the dependence of the up-converted signal at resonance frequency is less than 0.5 dB/50 mV @ 250 mV reverse bias, as it is seen in Fig. 15.

The level of the up-converted signal is dependent on the voltage of the local generator and the photo-voltage; thus, if we can increase these voltages, the mixing efficiency will be increased. The increase of the LO power (voltage) is easy, but the saturation limits this effect. The other way is to increase the photo-voltage by the double-mixing method. The optical detection using a p-i-n PD is based on an optical-power-to-electrical-current conversion. The photo-voltage is generated by the photocurrent converted from the optical power. If the impedance loading the "current generator" is small, the photo-voltage will be small, and if the impedance is high, the photo-voltage will be high as well. Using a resonant embedding circuit, this impedance can be set higher, and the mixing product will be higher. This method can be used easily, especially in the optical–microwave mixing method.

IV. Photodetection Investigation

First, the optical detection was characterized. The investigated PD was a MITEL 1A358 type CATV p-i-n PD ($C \cong 1.2$ pF, $R = 0.8$ A/W). The detection response was used as a reference. In this arrangement, the dynamic behavior of the PD was investigated in its detection mode of operation. The measurement setup is shown in Fig. 4. The intensity-modulated optical signal is generated by an HP 83424A 1550-nm distributed feedback (DFB) laser source and an HP 83422A external Mach–Zehnder optical modulator. The modulator was used with "MAX" modulation depth mode, and the built-in automatic gain control guaranteed the constant optical modulation depth (OMD).

The photodetected intensity-modulated optical signal was measured by a spectrum analyzer, and the result is shown in Fig. 5. The parameter of the surface is the reverse-bias voltage of the PD; it was varied in the range $0 \ldots 1.5$ V in 0.1-V steps. The frequency scale is multiplied by -1 so that the detection can be compared with the figures of mixing properties (see subsequently). Applying higher negative-bias voltages, the flatness of the curves is improved or, in other words, the frequency dependence is reduced.

V. Up-Conversion Investigation With a Circulator

The investigated optical–microwave mixing setup is shown in Fig. 6. The LO signal is fed to the PD via a circulator. The up-converted mixing product generated in the diode is measured by a spectrum analyzer. At the electrical connection of the PD, a wide-band circulator is used separating the input LO signal and the output up-converted signal.

The measured lower sideband of the up-converted signal is shown in Fig. 7. The intensity-modulated optical signal was generated by the same optical configuration as in the detection investigation. The circulator has a bandwidth of 2–4 GHz. The optical carrier was modulated by a $f_{\rm mod} = 10$–410-MHz signal. The LO signal has 0-dBm power at a 2.5-GHz frequency. The reverse bias of the PD was varied in the range 0–1.5 V in 0.1-V steps. In Fig. 7, the horizontal axis of the surface plot is the frequency offset from the 2.5-GHz carrier, the perpendicular axis shows the reverse bias of the PD, and the vertical scale is the power level of the up-converted signal.

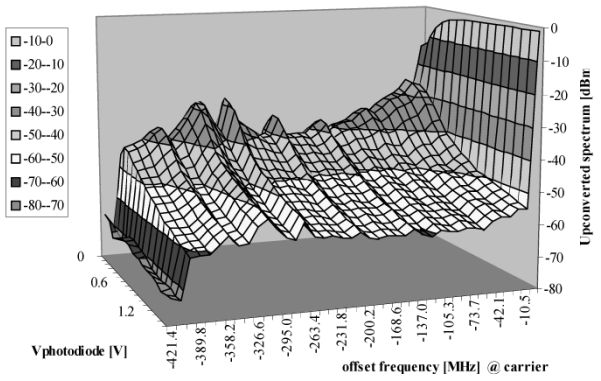

Fig. 7. Lower sideband of the up-converted signal (maximum −27.46 dBm @ 312 MHz).

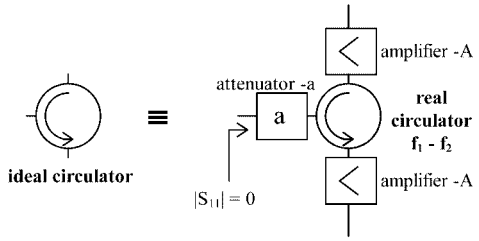

Fig. 8. "Ideal" circulator realization (approximately).

Outside its bandwidth, the circulator cannot produce a proper matching. Because the frequency of the baseband signal (detected signal) is lower than the band of the circulator (2–4 GHz), the PD sees a varying impedance in the baseband. The effect of this reflection is well seen in Fig. 7, causing the ripples.

If the length of the transmission line (semi-rigid) is about 8 cm, the up-converted spectrum has a −27.46-dBm peak at 312 MHz (if the length changes, the peak changes as well). Using this configuration, a mixing gain can be achieved. The gain compared with the detected signal is 8 dB, but the location of the resonance cannot be designed well.

VI. Up-Conversion Setup With "Ideal" Circulator

As it was shown, the resonance peaks were caused in the up-converted spectrum by the improper matching of the circulator in the band of the baseband signal. The real circulator can be completed by a simple circuit to achieve better matching in a wider band (see Fig. 8).

If the attenuation of the attenuator is sufficiently large, the reflection of the port connected to the PD is close to zero. If the amplification (A) is equal to the attenuation (a) the behavior of the real circulator is almost equal to the "ideal" one. The measurement of the optical–microwave mixing was repeated with the same setup by changing the circulator to an "ideal" one (using a 10-dB attenuator). (In the measurement, the amplifiers were left out, compensating their effects by the increased power of the LO signal and the shifted reference level of the spectrum analyzer.) The lower sideband of the up-converted spectrum is shown in Fig. 9 with the same settings as in the latter cases.

As it can be seen, the ripples in the spectrum are almost eliminated. Apart from the ripples, the form of the surface is approximately the same as in the real circulator case. The surface has a maximum edge at 0.2-V reverse-bias voltage.

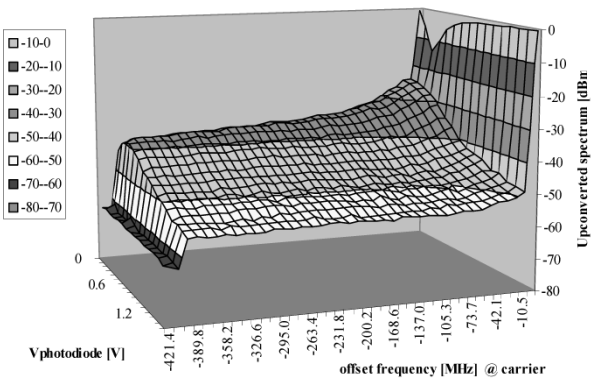

Fig. 9. Lower sideband of the up-converted signal mixing setup with "ideal" circulator.

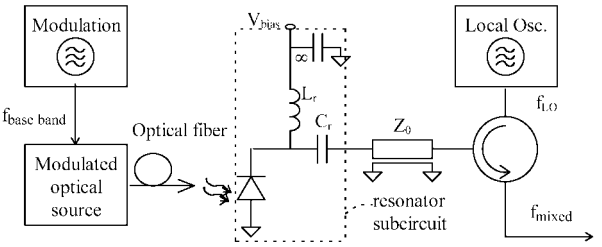

Fig. 10. Mixing measurement setup with an *LC* resonator.

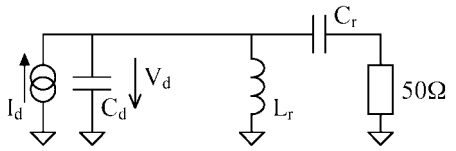

Fig. 11. Small-signal equivalent of the *LC* resonator.

VII. Up-Conversion Investigation With an Electrical *LC* Resonator

In some cases, the mixing gain effect—which overcomes the detected output power—is advantageous. For a suitable application, the simple design and the tuning of the resonance frequency have to be solved. The insufficiently well-defined location of the resonance using a real circulator setup can be eliminated by applying properly designed baseband resonator circuits. The developed resonator circuit is shown in Fig. 10. The embedding resonator circuit consists of a series capacitor and a parallel inductor (in the small-signal equivalent). At the frequency band of the up-converted signal, the inductor (L_r) is an open circuit, and the capacitor (C_r) is a small-series attenuator, so their effects can be neglected.

In the baseband, the capacitor can be approximated with an open circuit; thus, the PD is parallel-connected to the resonator inductance and a high impedance (series connection of the resonator capacitor C_r and the Z_0 system impedance), as shown in Fig. 11. These embedding circuit elements make a resonance with the capacitance of the photodiode.

The lower sideband of the up-converted spectrum is shown in Fig. 12 using the same signal properties as in the latter setups.

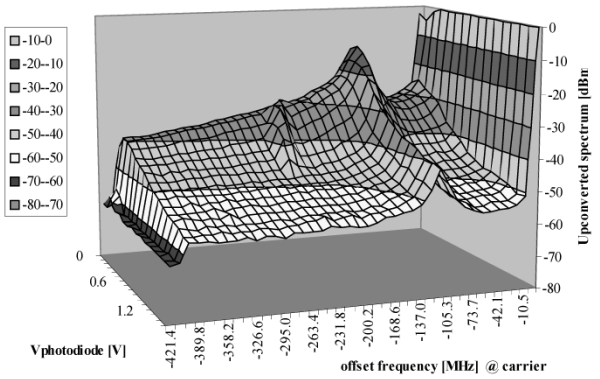

Fig. 12. Lower sideband of the up-converted signal (maximum −1.94 dBm @ 104 MHz).

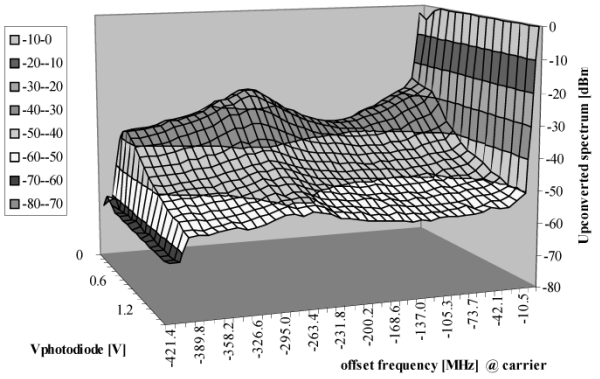

Fig. 13. Lower sideband of the up-converted signal (maximum −25.23-dBm @ 250 MHz).

In the measurement, a so-called "ideal" circulator was used to reduce the resonance effects of a real circulator disturbing the presentation of the *LC* resonance effect. The capacitance of the resonator capacitor is 4.7 pF, the equivalent capacitance of the PD is approximately 1 pF, and the resonator inductance was realized by a ten-loops inductor.

The surface has a maximum edge at about 0.2-V reverse-biased voltage. As it can be seen, the up-converted signal overcomes the detected signal in a narrow band. It has a resonant − 11.94-dBm high peak at 104 MHz. The mixing gain compared with the detected signal is about 24 dB. The advantage of the *LC* resonator method opposite to the resonance caused by the circulator is the well-defined and easily designed resonance frequency.

The frequency of the resonance can easily be changed by tuning the resonator inductor. If t a lower value for the inductor is set, the resonance frequency will be higher, as seen in Fig. 13 (the resonator inductance was realized by a three-loops inductor).

In Fig. 13, the resonance frequency is 250 MHz, and it has a −25.23-dBm peak. The peak is smaller, and the bandwidth around the peak is wider than in the case of a lower frequency resonance (Fig. 12). These effects are caused by the decreased transformed termination impedance (Z_0) through the resonator capacitor. The lower real part of the impedance decreases the

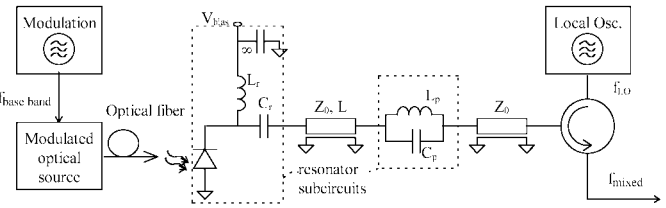

Fig. 14. Mixing measurement setup with series and parallel resonators.

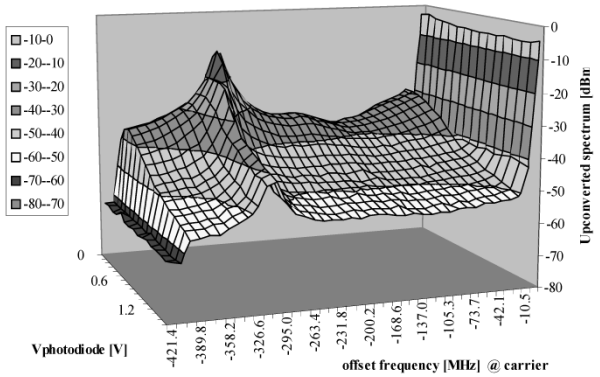

Fig. 15. Lower sideband of the up-converted signal using series and parallel resonances (maximum −10.86dBm @ 289 MHz).

effect of the resonance by reducing the quality factor of the resonator. That effect can be reduced by decreasing the capacitance, but in this case, the attenuation at the LO band will increase, causing a decrease in the up-converted output power. Due to these opposite effects, there is an optimum for the series resonator capacitance.

VIII. Up-Conversion Using Series and Parallel Resonances

The opposite effect of the resonator capacitor can be eliminated by using a developed new optical microwave configuration setup, shown in Fig. 14. The resonator is completed by a new resonator (L_p, C_p) in the series branch. This resonator is tuned to the resonance (baseband), and in a narrow band determined by the quality factor of the resonator, it shows a high input impedance; thus, it separates the PD from the Z_0 system impedance.

Applying this configuration, there is no decrease in the resonant peak at higher frequencies. A measured result can be seen in Fig. 15. The power of the 2.5-GHz LO signal is 0 dBm, as in the latter cases. The up-converted spectrum has a −10.86-dBm peak at the modulation frequency of 290 MHz. This peak overcomes the detected level by 25 dB.

The 3-dB bandwidth of the mixing product is 12 MHz in the present case. The mixing gain can be increased with higher resonator Q, but it results in a narrower bandwidth. The achievable gain is theoretically limited by the loss of the PD.

The LO power dependence of the up-converted spectrum was also investigated. At a higher $(> 5$ dBm$)$ LO signal level, a saturation effect can be observed. The lower sideband of the up-converted spectrum close to the saturation can be seen in Fig. 16. The LO power level is 5 dBm, and the other settings are the same as in the latter investigations.

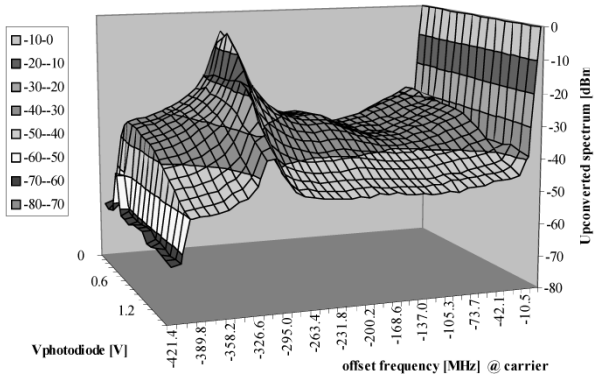

Fig. 16. Lower sideband of the up-converted signal using series and parallel resonances. $P_{\rm LO} = 5$ dBm (maximum $-$ 2.89 dBm @ 289 MHz).

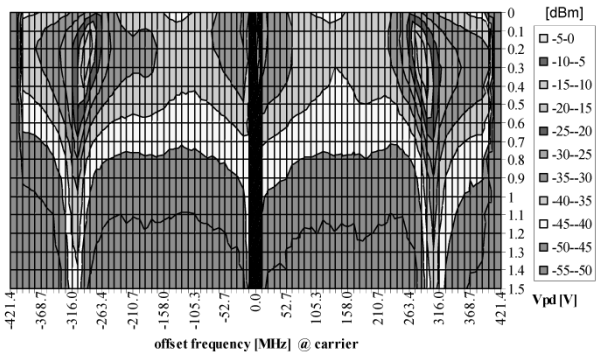

Fig. 17. Contour map of the up-converted spectrum. $P_{\rm LO} = 0$ dBm (maximum $-$ 10.86 dBm @ 289 MHz).

The spectrum shown in Fig. 16 has a $-$2.89-dBm peak at 289 MHz. This peak overcomes the detection by 33 dB, which is quite a significant mixing gain.

The contour map of the up-converted spectrum shown in Fig. 15 is plotted in Fig. 17. The figure shows both the lower and upper sidebands of the up-converted signal. As it can be seen, the lower and upper sidebands are almost symmetrical to each other.

The resonance frequency is shifted down by decreasing the reverse-bias voltage of the PD. The reason for this effect is that at lower reverse-bias voltage, the PD equivalent capacitance is higher so that the resonance frequency is shifted down.

IX. Transmission Properties

A. Noise Properties

The noise properties of the optical–microwave mixing effect were also investigated. Utilizing the reflection in mixing, the signals are superposed in phase, but because the noise sources are incoherent, a noise reduction has been expected. The output noise spectral density of the optical–microwave mixer is $-$141.7 dBm/Hz in the resonance band using a real circulator and 0- dBm LO power along with a 270-μW illumination without modulation. The noise of the p-i-n diode is relatively small because it works with reverse-bias voltage, and therefore, the dark current is very low. This way, the noise generated in the p-i-n diode is negligible to the noise contribution of other system components.

The noise density in the dark case is 0.58 dB higher than the thermal noise of the system. The slight noise increase can be explained by the relative intensity noise caused by the laser source and the external modulator. In spite of the increase in the noise spectral density, the signal-to-noise ratio is improved due to the high gain of the mixing effect.

In case of optical–electrical conversion, there is no conversion gain; however, a significant conversion loss is encountered. Therefore, the noise figure is basically determined by the conversion loss. As the optical–microwave double mixing approach exhibits much smaller conversion loss than the conventional mixing or the direct optical detection, the noise figure is significantly improved. That is a very important advantage in receiver applications.

B. Bandwidth

The bandwidth is basically dependent on the Q factor of the baseband resonator. With a higher Q factor, the bandwidth will be narrower; however, the transmission peak will be higher. That means there is a strong relationship between these two properties: when the transmission peak is higher, the bandwidth is narrower. However, it is possibile to broaden the band and keep the transmission peak unchanged by the application of more complex circuitry in the baseband, which has filter characteristics.

The optical–microwave double mixing has further advantages in receiver applications. As the received signal is converted into the intermediate frequency band, the electronic circuitry of the receiver will have a narrower relative bandwidth. Consequently, their transmission characteristics—like amplitude and group-delay responses—can be improved in the narrower relative bandwidth. Furthermore, the optical–microwave double mixing exhibits a filtering effect as well, which is very useful in the reception of subcarrier-multiplexed optical signals.

C. Operation Frequency

As it has already been shown, the operation frequency is mainly determined by the baseband circuit. However, the same mixing approach can be used at higher frequencies, but because the available gain is limited by the losses of the PD and the embedding resonant circuit, monolithic realization is proposed, which minimizes the parasitic effects. This way, the operation frequency can be shifted to higher frequencies, when the microwave monolithic integrated circuit (MMIC) construction is applied. Naturally, the Q factor of MMIC resonators is not so high as that of the lower frequency resonators utilizing lumped elements. Therefore, the height of the transmission peak is reduced when the operation frequency is increased.

X. Selective Reception of a Subcarrier Channel

In the presently used optical systems, the reception of modulated subcarrier signals is performed—after optical detection—in two different ways [19].

1) The subcarriers are separated by a series of fixed-frequency filters, and the wanted subcarrier is selected by a switch, which is a very complicated and expensive method.

2) A specific subcarrier is selected by a tuned filter. In this case, keeping the performance of the filter unchanged when it is tuned is very difficult because several resonators and their couplings are to be simultaneously controlled.

The selective-reception method of the present paper offers new perspectives. In the subcarrier-type optical communications, each transmitter has its own subcarrier frequency. The transmission capacity of the network can be increased by applying new subcarriers and, thus, the digital processing rate per subcarrier remains fixed.

Utilizing the new method for the reception of the subcarrier-multiplexed optical signal transmission, a much simpler receiver structure and channel selection can be achieved. By tuning the resonant circuit, a specific subcarrier signal is separately received. That is a big advantage because, besides the significant increase in the received signal, the filtering effect is also utilized [20], [21]. As the bandwidth of the subcarrier channels is usually relatively small, the narrow bandwidth of the present approach does not cause any problem in the reception.

The new optical–microwave double -mixing method is very promising because it produces an up-converted signal more than 30 dB higher than the directly detected signal.

XI. Conclusion

Some experimental constructions were investigated for optical–microwave mixing method. A significant increase in the received signal is obtained by applying the new optical–microwave double-mixing approach. In a narrow-band, a 30-dB-higher mixing product is obtained. The new method can be advantageously used for the reception of subcarrier-multiplexed optical signals.

Acknowledgment

The authors would like to acknowledge the Commission of the European Union and the Hungarian National Scientific Research Foundation for their support.

References

[1] T. T. Y. Wong, *Fundamentals of Distributed Amplification*. Boston, MA: Artech House, 1993.

[2] C. S. Aitchison, "The intrinsic noise figure of the MESFET distributed amplifier," *IEEE Trans. Microwave Theory Tech.*, vol. 33-MTT, pp. 460–466, June 1985.

[3] H. Ogawa, S. Banba, E. Suematsu, H. Kamitsuna, and D. Polifko, "A comparison of noise performance between a PIN diode and MMIC HEMT and HBT optical receivers," in *IEEE MTT-S Int. Microwave Symp. Dig.*, vol. 1, Atlanta, GA, June 1993, pp. 225–228.

[4] Q. Z. Liu, R. Davies, and R. I. MacDonald, "Experimental investigation of fiber optic microwave link with monolithic integrated optoelectonic mixing receiver," *IEEE Trans. Microwave Theory Tech.*, vol. 43, pp. 2357–2360, Sept. 1995.

[5] A. Paolella, S. Malone, T. Berceli, and P. R. Herczfeld, "MMIC compatible lightwave-microwave mixing technique," *IEEE Trans. Microwave Theory Tech.*, vol. 43, pp. 518–522, Mar 1995.

[6] T. Berceli, B. Cabon, A. Hilt, and G. Járó, "Improved optical-microwave mixing process utilizing high-speed photo-diodes," in *Proc. 26th Eur. Microwave Conf.*, vol. 1, Prague, Czech Republic, Sept. 1996, pp. 125–129.

[7] H. Ogawa and Y. Kamiya, "Fiber-optic microwave transmission using harmonic laser mixing, optoelectronic mixing, and optically pumped mixing," *IEEE Trans. Microwave Theory Tech.*, vol. 39, pp. 2045–2051, Dec. 1991.

[8] C. P. Liu, Y. Betser, A. J. Seeds, D. Ritter, and A. Madjar, "Optoelectronic mixing in three-terminal InP/InGaAs heterojunction bipolar transistors," in *IEEE MTT-S Int. Microwave Symp. Dig.*, vol. 1, June 1997, pp. 359–362.

[9] N. J. Gomes and A. J. Seeds, "Tunnelling metal-semiconductor contact optically pumped mixer," *Optoelectronics IEE Proc. J.*, vol. 136, no. 1, pp. 88–96, Feb. 1989.

[10] H. Kamitsuna and H. Ogawa, "Fiber optic microwave links using balanced/image canceling photo-diode mixing," *IEICE Trans. Electron.*, vol. E76-C, no. 2, pp. 264–269, Feb. 1993.

[11] Q. Z. Liu, R. Davies, and R. I. MacDonald, "Fiber optic microwave link with monolithic integrated optoelectonic up-converter," *IEEE Photon. Technol. Lett.*, vol. 7, pp. 567–569, May 1995.

[12] A. J. Seeds, "Microwave photonics," *IEEE Trans. Microwave Theory Tech.*, vol. 50, pp. 877–887, Mar. 2002.

[13] J. E. Bowers, C. A. Burrus, and R. J. McCoy, "InGaAs PIN photodetectors with modulation response to millimeter wavelengths," *Electron. Lett.*, vol. 21, no. 18, pp. 812–814, Aug. 1985.

[14] A. Stolze and G. Kompa, "Nonlinear modeling of dispersive photodiodes based on frequency- and time-domain measurements," in *Proc. 26th EUMC*, Prague, Czech Republic, Sept. 1996, pp. 379–382.

[15] R. Sabella and S. Merli, "Analysis of InGaAs P-I-N photodiode frequency response," *IEEE J. Quantum Electron.*, vol. 29, pp. 906–916, Mar. 1993.

[16] G. Járó, T. Berceli, A. Hilt, and A. Zólomy, "New optomixer surpassing photodetection at microwaves," in *Tech. Dig. Int. IEEE MTT-S Topical Meeting Microwave Photonics*, Duisburg, Germany, Sept. 1997, pp. 143–146.

[17] K. J. Williams, R. D. Esman, and M. Dagenais, "Nonlinearities in P-I-N microwave photodetectors," *J. Lightwave Technol.*, vol. 14, pp. 84–96, Jan. 1996.

[18] T. Berceli, B. Cabon, A. Hilt, A. H. Quoc, É Pic, and S. Tedjini, "Dynamic characterization of optical—Microwave transducers," in *IEEE MTT-S Int. Microwave Symp. Dig.*, vol. 3, Orlando, FL, May 1995, pp. 1295–1298.

[19] U. Gliese, "Multifunctional fiber—Optic microwave links based on remote heterodyne detection," *IEEE Trans. Microwave Theory Tech.*, vol. 46, pp. 458–468, May 1998.

[20] T. Marozsák, E. Udvary, and T. Berceli, "A combined optical—Wireless broadband Internet access: Transmission challenges," in *IEEE MTT Int. Microwave Symp. Dig.*, Phoenix, AZ, May 2001, pp. 997–1000.

[21] T. Marozsák, A. Kovács, E. Udvary, and T. Berceli, "Direct modulated lasers in radio over fiber applications," in *Proc. Microwave Photonics, MWP 2002*, Awaji, Japan, Nov. 2002, pp. 129–132.

Gábor Járó (M'03) received the M.Sc. degree in electrical engineering, with a thesis titled "Development of an X-Band Scatterometer," and the Ph.D. degree, based on his dissertation titled "High Speed Optical Receivers," both from the Technical University of Budapest, Hungary.

He was an Assistant Professor at the Technical University of Budapest for two years. He is currently working for Nokia Hungary, Budapest, Hungary. His research interest is in the areas of noise in high-speed optical receivers and millimeter-wave signal generation in optical systems.

Tibor Berceli (SM'77–F'94) was a Visiting Professor in the United States, United Kingdom, Germany, France, Finland, and Japan. He is currently Professor of Electrical Engineering at the Budapest University of Technology and Economics, Budapest, Hungary. He instructs eight Ph.D. students and works on several European projects. He has published more than 170 papers in the field of microwave and optical communications and has written six books and received 26 patents. His present research activity is in microwave photonics.